

Contents lists available at [ScienceDirect](https://www.sciencedirect.com)

Crop and Environment

journal homepage: www.journals.elsevier.com/crop-and-environment

Original Article

Sensor-based measurements of NDVI in small grain and corn fields by tractor, drone, and satellite platforms

Jarrod O. Miller^{a,*}, Pinki Mondal^{a,b}, Manan Sarupria^b^a Department of Plant and Soil Sciences, University of Delaware, Newark 19716, USA^b Department of Geography and Spatial Sciences, University of Delaware, Newark 19716, USA

ARTICLE INFO

Keywords:

Corn
Drone
NDVI
Nitrogen
Satellite
Small grains

ABSTRACT

The use of sensors for variable rate nitrogen (VRN) applications is transitioning from equipment-based to drone and satellite technologies. However, regional algorithms, initially designed for proximal active sensors, require evaluation for compatibility with remotely sensed reflectance and N-rate predictions. This study observed normalized difference vegetation index (NDVI) data from six small grain and two corn fields over three years. We employed three platforms: tractor-mounted active sensors (T-NDVI), passive multispectral drone (D-NDVI), and satellite (S-NDVI) sensors. Averaged NDVI values were extracted from the as-applied equipment polygons. Correlations between NDVI values from the three platforms were positive and strong, with D-NDVI consistently recording the highest values, particularly in areas with lower plant biomass. This was attributed to D-NDVI's lower soil reflectance and its ability to measure the entire biomass within equipment polygons. For small grains, sensors spaced on equipment booms might not capture accurate biomass in poor-growing and low NDVI regions. Regarding VRN, S-NDVI and D-NDVI occasionally aligned with T-NDVI recommendations but often suggested half the active sensor rate. Final yields showed some correlation with landscape variables, irrespective of N application. This finding suggests the potential use of drone or satellite imagery to provide multiple NDVI maps before application, incorporating expected landscape responses and thereby enhancing VRN effectiveness.

1. Introduction

The decline in water quality due to nutrient pollution can be tempered by field management techniques to reduce nutrient export (Ator et al., 2020; Beegle, 2013). Precision nitrogen (N) management, including the use of in-season canopy reflectance, can provide environmental benefits through reduced postharvest N (Roberts et al., 2010). Proximal canopy sensors have been used to improve N use efficiency for field crops by estimating in-season crop needs and addressing landscape variability (Aula et al., 2020; Cao et al., 2017; Erdle et al., 2011). Reductions in N application have been performed without reducing crop yield (Aula et al., 2020; Barker and Sawyer, 2012) while providing lower greenhouse gas emissions (Cao et al., 2017).

Although initial work in crop sensing was performed with passive sensors, tractor-mounted active canopy sensors were developed for variable rate N (VRN) applications (Barker and Sawyer, 2010; Samborski et al., 2009). Active sensors have their own light source and do not have to rely on external light sources (e.g. sunlight) to obtain plant reflectance (Holland et al., 2012; Winterhalter et al.,

2013). Light reflected from plants includes wavelengths in bands such as green, red, and near-infrared (NIR), where healthy biomass reflects green and NIR light while absorbing red and blue light (Inman et al., 2005a). Indices have been developed using specific wavelengths, such as the normalized difference vegetation index (NDVI), to estimate plant biomass (Dellinger et al., 2008; Holland et al., 2012; Raun et al., 2005b). NDVI can be strongly correlated to vegetative biomass (Solie et al., 2012) but not necessarily nutrient content alone (Benincasa et al., 2018).

To overcome issues with the NDVI relationship to N content, VRN applications are based on algorithms that can include growing degree days (GDD), N-enriched strips, and the number of days from planting to improve estimations of yield potential (Franzen et al., 2016; Raun et al., 2005b). Other adjustments to sensor-based N management include the use of field management zones, pre-plant N, manure or legume credits, and contributions of N from irrigation (Fassa et al., 2022; Holland and Schepers, 2010; Thompson and Puntel, 2020). Whatever additional variables are used in an algorithm, sensor-based indices are a consistent component used to estimate plant N status (Franzen et al., 2016).

* Corresponding author.

E-mail address: Jarrod@udel.edu (J.O. Miller).

<https://doi.org/10.1016/j.crope.2023.11.001>

Received 5 July 2023; Received in revised form 11 November 2023; Accepted 12 November 2023

2773-126X/© 2023 The Author(s). Published by Elsevier Ltd on behalf of Huazhong Agricultural University. This is an open access article under the CC BY-NC-ND license (<http://creativecommons.org/licenses/by-nc-nd/4.0/>).

Regional algorithms have been developed from N-rate trials using sensors in Oklahoma (Raun et al., 2005b), Virginia (Thomason et al., 2011), and New York (Tagarakis and Ketterings, 2018).

With the recent adoption of drones (unoccupied aerial vehicles or UAV) in agriculture production, passive multispectral sensors are being examined to make VRN prescriptions (Benincasa et al., 2018; Heinemann et al., 2022; Mizuta et al., 2022; Sozzi et al., 2021; Walsh et al., 2018). There is potential for drone or satellite NDVI to be substituted within VRN models, but measured values may vary as passive sensors require ample sunlight which varies with solar angles, and their NDVI can change within a smaller range (Holland et al., 2012; Morris et al., 2018; Winterhalter et al., 2013). Questions also remain as to how similar drone or satellite-based vegetation indices may be substituted into established algorithms, particularly as algorithms were developed using active sensors measured directly along crop rows (Barker and Sawyer, 2010; Morris et al., 2018), potentially including more soil reflectance. Soil pixels can be removed from drone images during processing (Thompson and Puntel, 2020), which could be an advantage in small grains when sensors are not directly over the row (Morris et al., 2018). There are some known benefits to passive drone-mounted sensors, where they have had better relationships with wheat biomass, possibly due to the off-nadir measurements of ground-based sensors (Heinemann et al., 2022).

Sensor resolution will also vary among the different platforms, which may affect NDVI values or the amount of soil reflected. An active optical sensor may measure a 0.61×0.61 m area (Inman et al., 2005a), while passive sensors in satellites could range from 1 to 60 m in resolution (Benincasa et al., 2018; Yu et al., 2021). Drone-mounted multispectral cameras can vary in resolution based on flying height, for example, between 1.29 and 11.00 cm pixel⁻¹ when flown between 30 and 120 m above ground level (Miller and Adkins, 2021). However, the NDVI measured on small grains from different heights was not very different and was able to differentiate between different populations (Miller and Adkins, 2021).

The finer resolution of drone imagery may also provide a better understanding of how landscape variables relate to N response and the creation of management zones (Inman et al., 2005b; Thompson and Puntel, 2020). For corn and small grains, there has been a strong spatial dependence on N uptake and yield related to soil properties (Inman et al., 2005b; Raun et al., 2005b). The spatial variability in soil properties, including soil texture and moisture, can also have a temporal component, as soil properties have exhibited a greater influence on growth during dry years (Stadler et al., 2015). Temporal measurements may also be an advantage of drone and satellite platforms, where measuring the change in NDVI values over the growing season has been successful in relating biomass, growth, and yield (Miller and Adkins, 2021; Raun et al., 2001). Equipment-mounted sensors would need to be driven over the field repeatedly to perform the same function.

For use in established algorithms, one issue comparing remote and tractor-based sensing could be how similar NDVI values are between platforms since specific NDVI values are used to cut off N applications at high or low biomass (Thomason et al., 2011). There may also be variation in the NDVI of high- or low-N reference strips between platforms and sensors (Solie et al., 2012; Thomason et al., 2011), although individual field reference strips are designed to correct for local and annual conditions.

The objective of this study was to compare how drone and satellite multispectral sensors may substitute for a ground-based active NDVI sensor (Greenseeker™) using a Mid-Atlantic region algorithm for N recommendations. Our other objective was to observe how field maps with different resolutions may vary in their estimations of NDVI, leading to different recommendations for field-based VRN.

2. Materials and methods

2.1. Drone image collection

Fields were selected from a farmer cooperator in Talbot County, MD, who adopted a Greenseeker active optical sensor for VRN application to

small grains and corn. VRN applications were made by the cooperator using the algorithm designed by Virginia Tech (Thomason et al., 2011), using NDVI from high and low N rate strips, pre-plant N, days from planting, maximum yield, and a maximum (constrained) N rate as inputs. The application was made with a 27 m boom with six active sensors creating a 3.66 m length region on the boom for NDVI measurements, where the actual area depended on the length of the field driven. For small grain fields, communication was maintained with the cooperator to arrange for drone flights over each field prior to an application at Zadoks growth stage (GS) 23 and again at GS 30. A flat rate was made at GS 23, and the VRN application was made at GS 30. Due to weather restrictions on drone flights, including cloud cover and high winds (> 20 mph), flights were timed for sunny days close to the application dates (Table 1).

Drone flights were performed in 2019 with a Parrot Disco Pro Ag fixed wing drone equipped with a Parrot Sequoia multispectral camera (Fig. 1). The Sequoia can produce images in the red (R), green (G), red edge (RE), and NIR wavelengths. Flights in 2020 and 2021 were performed with a DJI Matrice 210 equipped with a Micasense Altum multispectral camera (Seattle, WA). The Altum can take images in the R, G, RE, and NIR bands but also includes imagery in the blue (B) wavelengths. Both cameras have GPS sensors that georeferenced each captured image. The GPS unit also has a sunshine sensor, which is placed on top of the drone and marks each image with data on lighting conditions. Flights were performed at 76 m above ground level which produced imagery with 7.16 and 3.28 cm pixel⁻¹ resolution in the Sequoia and Altum cameras, respectively. Image was captured at an 80% front overlap and 75% side overlap. Images of a calibration panel to correct for lighting conditions were taken before each flight to input into the photogrammetric software. Each year, ground control points (GCP) were placed prior to the flights and georeferenced (WGS84) using an Emlid Reach+ GPS receiver with RTK corrections provided wirelessly through Keynet.

2.2. Drone image processing

All images were stitched together using Pix4D Mapper photogrammetric software (Prilly, Switzerland), using the settings for multispectral cameras, and incorporating both calibration photos and the GCP. The only setting adjusted in Pix4D was to use “triangulation” to calculate the digital surface model (DSM), which is recommended for agricultural fields by Pix4D. The stitched NDVI orthomosaic and DSM produced by Pix4D were incorporated into ArcGIS Pro. Mounted active optical sensor readings were obtained from the cooperator as a polygon shapefile and overlaid on the drone orthomosaics. As the tractor-based optical sensor only measures NDVI, it was the only index calculated from multispectral drone imagery.

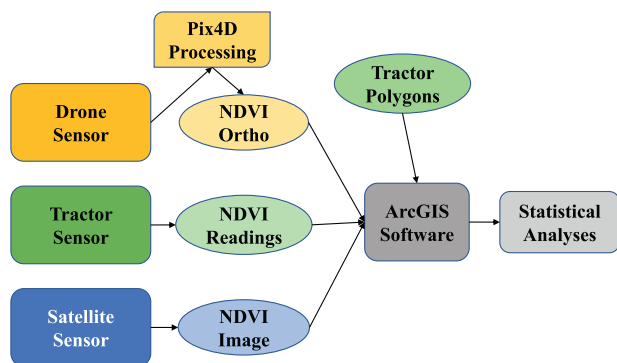
2.3. Satellite imagery processing

This study utilized the Level 2A products from the Copernicus Sentinel-2 mission to obtain NDVI values from satellite imagery. Developed by the European Space Agency (ESA), Sentinel-2 is a constellation of satellites that carries a MultiSpectral Instrument (MSI) and offers high-resolution optical images with a spatial resolution of 10–60 m and a temporal resolution of 5 d. The MSI sensor on board Sentinel-2 provides data in 13 bands, ranging from visible R, G, B, and NIR to shortwave infrared. We relied on Google Earth Engine (GEE), a freely available cloud-based platform for geospatial data processing, to acquire and process the Sentinel-2 images used in this study. Level-2A data are an advanced and analysis-ready rendition of the original Level-1C data. Level-2A data are atmospherically corrected, which effectively mitigates the impact of Earth's atmospheric constituents, notably aerosols, clouds, and water vapor. Consequently, Level-2A data characterize surface reflectance, quantifying the portion of solar irradiance reflected by the earth's surface. Additionally, Level-2A data also incorporate cloud mask information stored in the QA60 band, facilitating effective masking of

Table 1

Field names and dates for planting, tractor sensing, drone flights, and satellite imagery acquisitions.

Field	Planting date	Sensor acquisition dates				
		Satellite GS23	Drone GS23	Tractor GS30 ^a	Drone GS30	Satellite GS30
Barley19	10/02/2018	02/05/2019	NA ^b	04/08/2019	04/08/2019	04/06/2019
Wheat19	10/22/2018	02/05/2019	NA	04/9/2019	04/08/2019	04/06/2019
Wheat20A	10/14/2019	2/15/2020	2/21/2020	3/20/2020	3/22/2020	3/16/2020
Wheat20B	10/18/2019	2/15/2020	2/21/2020	3/20/2020	3/22/2020	3/16/2020
Barley21	10/07/2020	2/24/2021	2/17/2021	04/07/2021	04/05/2021	04/05/2021
Wheat21	10/28/2020	2/24/2021	2/17/2021	04/07/2021	04/05/2021	04/05/2021
Corn Rainfed	4/20/2020	NA	NA	6/22/2020	6/26/2020	6/24/2020
Corn Irrigated	5/14/2020	NA	NA	6/26/2020	6/26/2020	6/24/2020

^a Corn was at six leaf (V6) growth stage.^b Not applicable.**Fig. 1.** Workflow of NDVI collection and processing.

cloud cover across the study area. We used QA60 band to include pixels with no cloud cover.

The drone orthomosaics of all farm fields were imported as assets in GEE. The geometrical boundaries of the orthomosaics were used to clip the Sentinel-2 surface reflectance images to obtain data from the same field sites. Cloud-free Sentinel-2 images acquired closest to the date of the drone flights were used for the analysis (Table 1). The NDVI for each individual farm field raster was calculated using the NIR and R bands using the following equation:

$$NDVI = \frac{NIR - RED}{NIR + RED}$$

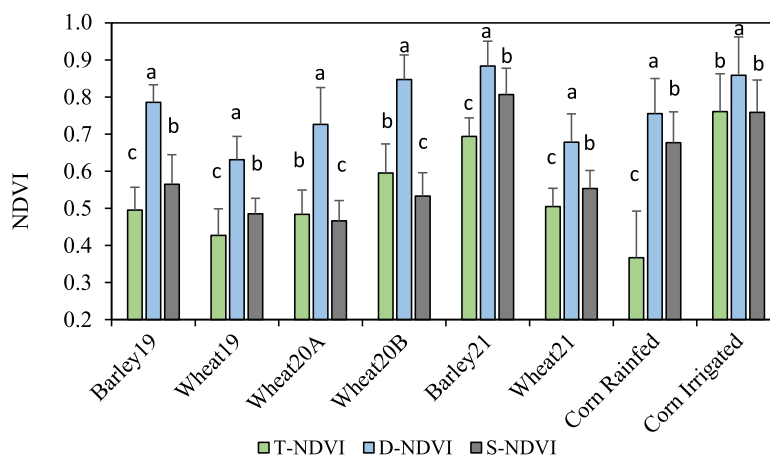
2.4. NDVI and landscape variable extraction

The raster calculator in ArcGIS Pro was used to subtract the GS 23 small grain NDVI (drone and satellite) from the GS 30 imagery to measure temporal differences between winter and early spring growth. From drone and satellite imagery, NDVI values were extracted using Zonal Statistics as Table with the as-applied polygon layer as the Feature Data/Mask. Tables were exported by the Table to Excel function. Equipment mounted (T-NDVI), drone mounted (D-NDVI), and satellite NDVI (S-NDVI) were matched in Excel using the as-applied polygon IDs. In Excel, T-NDVI was subtracted from D-NDVI and S-NDVI to measure the differences between them in each polygon.

Landscape variables were derived using 1 m digital elevation models (DEM) deriving from LiDAR provided by the state of Maryland for each county (Imap, 2022). Average elevation was extracted using the T-NDVI polygons from each DEM. Slope rasters were created for each field using the Slope function in ArcGIS spatial analyst. Topographic wetness index (TWI) was calculated using the following equation:

$$TWI = \ln \frac{a}{\tan b}$$

For the TWI calculation, *a* represents the local upslope drainage, whereas *b* is the slope in radians and is used to estimate parts of a landscape that may accumulate more water. For this calculation, the DEM was resampled to a 5 m resolution. Flow direction and flow accumulation were calculated using Spatial Analyst tools. Flow accumulation was scaled by adding one and multiplying by the cell size. The final TWI raster had values averaged using Zonal Statistics and the T-NDVI polygons.

**Fig. 2.** Field averaged NDVI from each field compared across the tractor based (T-NDVI), drone based (D-NDVI), and satellite based (S-NDVI) platforms using Tukeys LSD ($P = 0.05$). Differences are compared within each sampled field and values with different letters are significantly different.

To compare the average NDVI within each polygon, T-NDVI, D-NDVI, and S-NDVI values were compared in SAS using Proc GLM and Tukey's Least Significant Difference ($P = 0.05$). The SAS function Proc Corr was used to analyze correlations among yield, NDVI values, and landscape-derived variables..

3. Results

3.1. Comparisons of NDVI measured by sensors mounted on tractors, drones, or satellites

The highest small grain NDVI for all platforms was Barley21, while the lowest was Wheat19 (Fig. 2). Based on individual platforms, D-NDVI

had the highest value across all fields. Field averaged D-NDVI ranged from 0.08 to 0.39 units higher than T-NDVI and S-NDVI, with the largest difference between the drone and tractor in the rainfed corn field. The rainfed corn field also had the largest standard deviation for T-NDVI. For the irrigated corn field, D-NDVI was only 0.1 units higher than T-NDVI, while S-NDVI ranged from 0.08 to 0.10 units lower than D-NDVI in both corn fields.

The T-NDVI was only the lowest in five out of the seven fields sampled (Fig. 2). For the eighth field, which was irrigated corn, the measurements were similar between the T-NDVI and S-NDVI. The rainfed corn field also produced the highest difference between the T-NDVI and S-NDVI (0.31), while all other measurements ranged from 0.02 to 0.07.

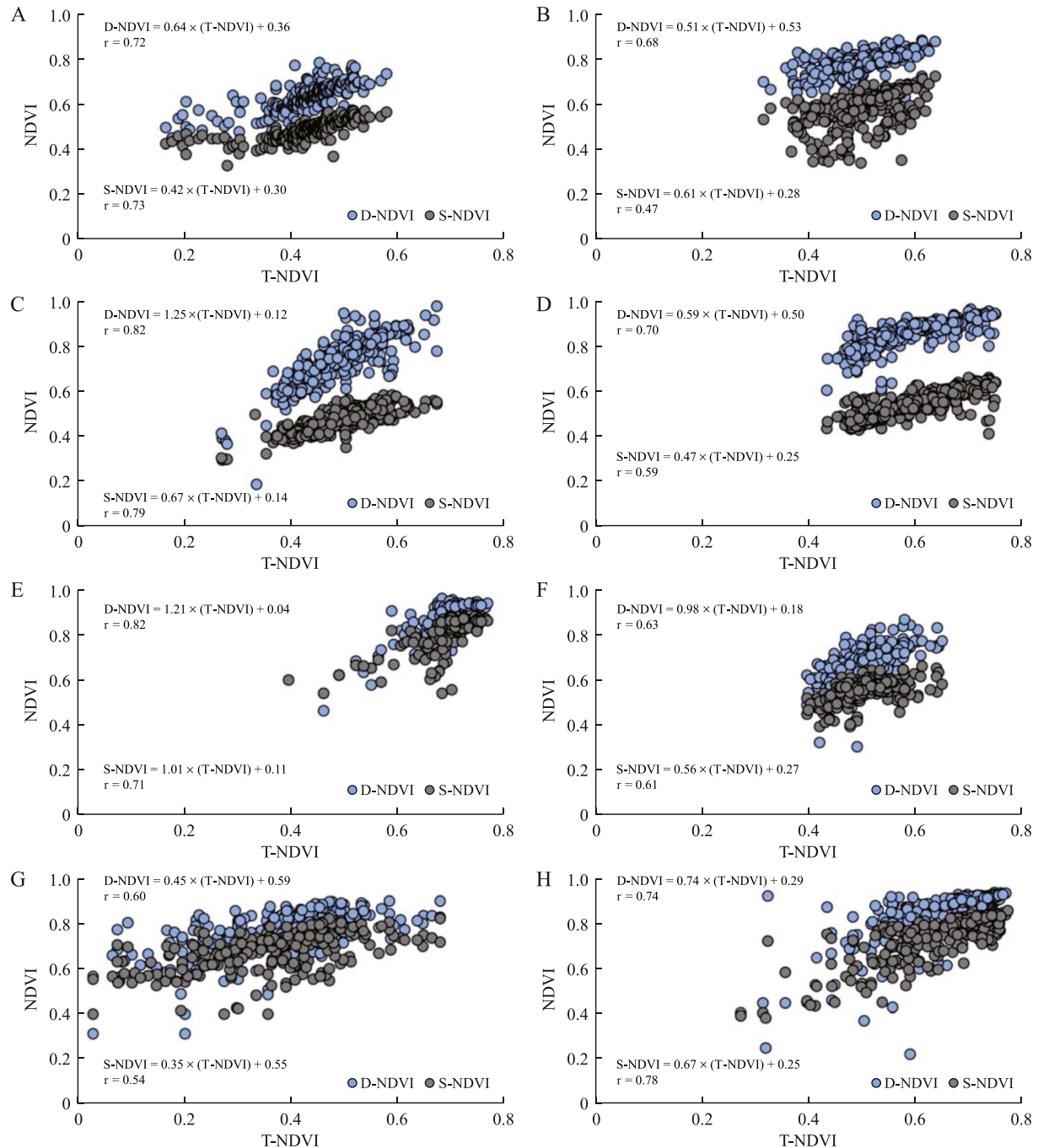


Fig. 3. Regression equations and Pearson correlation coefficients (r) between tractor based (T-NDVI) and drone based (D-NDVI) or satellite based (S-NDVI) NDVI for Wheat19 (A), Barley19 (B), Wheat20A (C), Wheat20B (D), Barley21 (E), Wheat21 (F), rainfed corn (G), and irrigated corn (H).

3.2. Relationships between T-NDVI, D-NDVI, and S-NDVI

When both D-NDVI and S-NDVI were regressed against T-NDVI, the relationships varied among fields (Fig. 3). The D-NDVI values were consistently higher than the S-NDVI values across all points sampled, with the largest difference in the slope of the relationship in Wheat20A and Wheat21. For small grain fields, except for Wheat19 the correlation coefficient values were greater for relationships with D-NDVI, with the largest difference in Barley19. Based on the slopes and intercepts of some of the regressions, larger discrepancies in T-NDVI and D-NDVI often occurred at lower values, with D-NDVI being 0.2 units higher at lower ranges (NDVI ranged from 0.30 to 0.40).

For small grains, correlations between D-NDVI and T-NDVI were consistently strong positive based on GS 30 with r ranging from 0.63 to 0.82 (Fig. 3), while correlation coefficient between S-NDVI and T-NDVI ranging from 0.47 to 0.79. For corn fields, the rainfed field had a lower correlation between D-NDVI and T-NDVI ($r = 0.60$) than the irrigated field ($r = 0.74$), but D-NDVI and S-NDVI had stronger relationships (r values ranged from 0.84 to 0.88).

3.3. Estimating N-rates between T-NDVI, D-NDVI, and S-NDVI measurements

Using the regression equations, T-NDVI values for target NDVI (0.50), low reference NDVI (0.30), and high reference NDVI (0.80) were used to estimate the same values for both D-NDVI and S-NDVI (Table 2). The largest discrepancy was often in the low reference strip values, with D-NDVI up to 0.39 units higher in Barley19 but only 0.10 units higher in Barley21. S-NDVI estimates were much closer to the T-NDVI low reference values, being only 0.04–0.16 units higher for small grains. The high NDVI reference strips were sometimes lower for S-NDVI but always higher for D-NDVI. For the corn fields, larger discrepancies in NDVI were observed in the rainfed than in the irrigated corn fields.

These values were used in the Virginia Tech algorithm to estimate potential N rates (Table 2), which were 101 kg ha⁻¹ for small grain fields, 213 kg ha⁻¹ for rainfed corn fields, and 297 kg ha⁻¹ for the irrigated corn field for T-NDVI. The D-NDVI was able to predict the same N rate for Wheat19, Barley21, and Wheat21. The S-NDVI rates were similar for two different fields (Barley19 and Wheat20A) and predicted the same as D-NDVI for Barley21. Otherwise, the rates were 45–82% of the suggested T-NDVI rates for small grains for both D-NDVI and S-NDVI. For the rainfed corn field, D-NDVI and S-NDVI made recommendations that were 64% and 69% of the T-NDVI rate, respectively. For irrigated corn, the S-NDVI estimated about 79% of the irrigated corn rate, while D-NDVI was much closer at 96%.

3.4. Relationships between landscape variables and measured NDVI

For T-NDVI, elevation had no relationships in irrigated corn fields and mixed relationships with small grains (Table 3). The strongest relationship was for Barley19, which was $r = -0.34$. Where it was significant,

slope had consistently negative relationships with T-NDVI, with the strongest relationship also in field Barley19. TWI had very low relationships with T-NDVI, but they were positive where presented, also with the strongest relationship in field Barley19.

The D-NDVI and S-NDVI mirrored the relationships observed above, with Wheat20B and Barley21 having the only positive relationships between NDVI and elevation (Table 3). Where significant, slope was related to lower NDVI in drone and satellite-based measurements, and field Barley19 had the strongest negative correlation. More fields had significant positive correlations between S-NDVI and TWI than those based on drones or tractors, although they were all weak (r ranged from 0.14 to 0.28).

Drone imagery and contours reveal where TWI may have more influence, with depressions in Wheat19, Wheat20A, and the irrigated corn field all collecting moisture. For the irrigated corn field (Fig. 4H) and Wheat20A (Fig. 4C), these depressions were in upland locations, while the Wheat19 (Fig. 4A) field had depressions at lower elevations where winter saturation killed the small grain crop.

Drainage also played a role in crop growth due to slopes, as steeper slopes (evident where there were closer contours) in Barley19 (Fig. 4A) and Wheat20A (Fig. 4C) reduced growth. The very low NDVI values observed in the rainfed corn field (Fig. 4G) were at the edges of the field and along drainage ditches. This was the same field sampled for Barley21 (Fig. 4E), where the drainage ditch also reduced small grain growth.

Due to the spacing of active sensors on the sprayer boom, some of the very low T-NDVI (NDVI < 0.1) readings were along the field edges.

Table 3

Pearson correlation coefficients between NDVI and field characteristics. NDVI were tractor based (T-NDVI), drone based (D-NDVI), and satellite based (S-NDVI) and field characteristics included elevation, slope, and topographic wetness index (TWI).

	Elevation	Slope	TWI	Elevation	Slope	TWI
	<i>Barley19</i>			<i>Wheat19</i>		
T-NDVI	-0.34	-0.51	0.46	NS ^a	-0.18	NS
D-NDVI	-0.31	-0.55	0.45	-0.22	-0.20	NS
S-NDVI	-0.26	-0.26	0.20	-0.26	-0.26	0.20
	<i>Wheat20A</i>			<i>Wheat20B</i>		
T-NDVI	-0.30	-0.10	0.13	0.16	NS	NS
D-NDVI	-0.29	-0.18	0.18	0.19	NS	NS
S-NDVI	-0.31	-0.15	0.18	0.32	NS	0.28
	<i>Barley21</i>			<i>Wheat21</i>		
T-NDVI	0.21	-0.16	NS	-0.25	NS	0.16
D-NDVI	0.24	-0.27	NS	-0.26	NS	0.13
S-NDVI	NS	-0.17	NS	-0.36	NS	0.14
	<i>Corn Rainfed</i>			<i>Corn Irrigated</i>		
T-NDVI	0.21	-0.16	NS	NS	NS	NS
D-NDVI	-0.18	NS	NS	NS	-0.16	-0.09
S-NDVI	-0.21	NS	NS	NS	NS	NS

^a No significant difference at $P = 0.05$.

Table 2

Estimated NDVI values using the relationship between tractor based (T-NDVI), drone based (D-NDVI), and satellite based (S-NDVI) for the target application (T-NDVI = 0.50), low reference strip (T-NDVI = 0.30), and high reference strip (T-NDVI = 0.80) and resulting N recommendation (tractor based = 101 kg ha⁻¹ for small grains, 213 kg ha⁻¹ for rainfed corn, and 297 kg ha⁻¹ for irrigated corn).

Field	Target NDVI		Low NDVI		High NDVI		N rate (kg ha ⁻¹)	
	D-NDVI	S-NDVI	D-NDVI	S-NDVI	D-NDVI	S-NDVI	D-NDVI	S-NDVI
Barley19	0.79	0.58	0.69	0.46	0.94	0.76	57	101
Wheat19	0.68	0.52	0.55	0.43	0.87	0.64	101	45
Wheat20A	0.75	0.48	0.49	0.34	0.99 ^a	0.68	83	101
Wheat20B	0.79	0.49	0.67	0.39	0.97	0.63	56	45
Barley21	0.65	0.61	0.40	0.41	0.99 ^a	0.91	101	101
Wheat21	0.67	0.55	0.47	0.43	0.97	0.72	101	81
Corn Rainfed	0.82	0.72	0.72	0.65	0.95	0.83	136	147
Corn Irrigated	0.66	0.59	0.52	0.45	0.89	0.78	284	234

^a The value 0.99 is used where estimates were over 1.0.

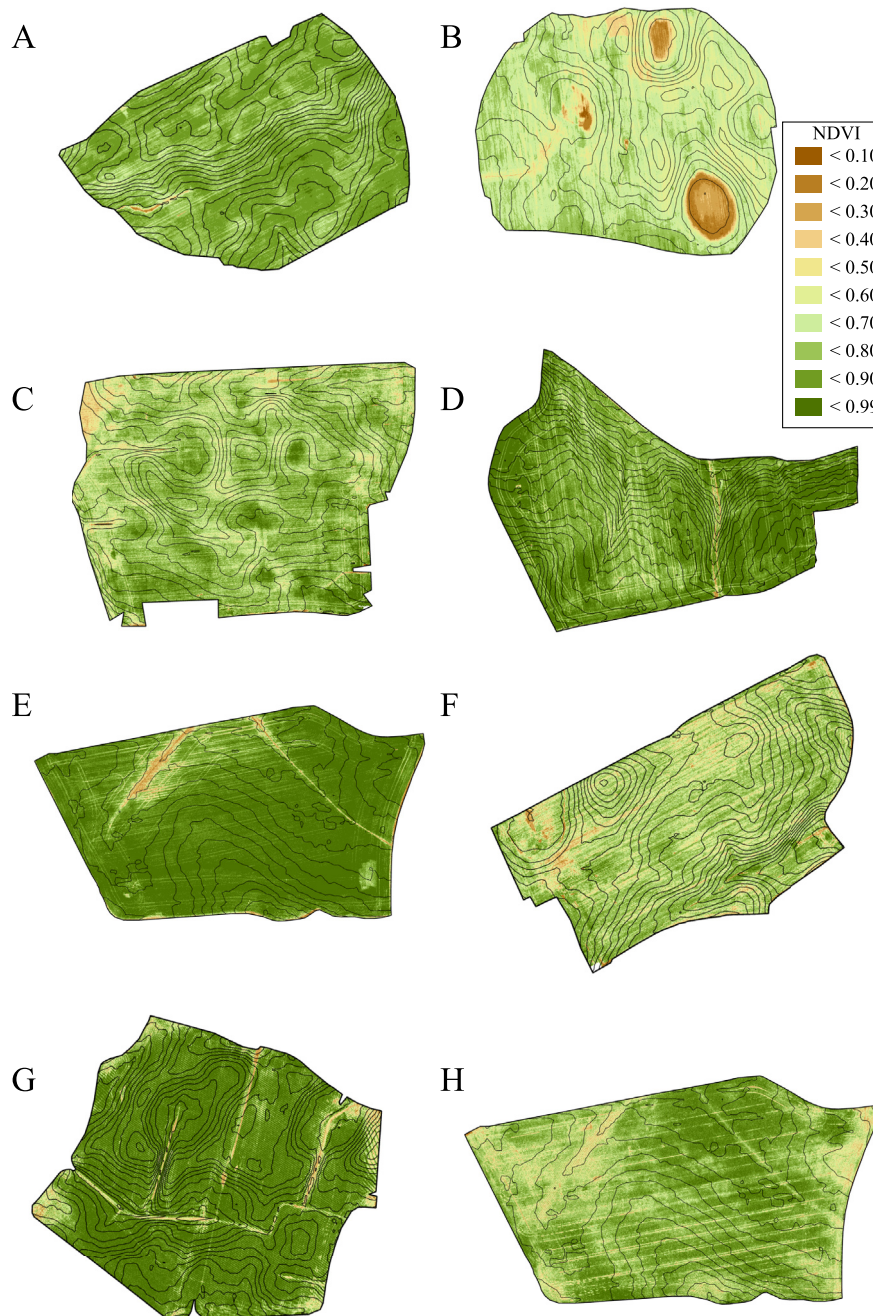


Fig. 4. Drone-derived NDVI overlain by 0.2 m elevation contours for the Wheat19 (A), Barley19 (B), Wheat20A (C), Wheat20B (D), Barley21 (E), Wheat21 (F), rainfed corn (G), and irrigated corn (H).

Since the application equipment had automatic section control, overlapping polygons, or those along depressions lacking in growth (Wheat19), recorded a larger area than their applied N. However, D-NDVI and S-NDVI measurements were only extracted from the as-applied polygons.

3.5. Relationships between yield and NDVI or landscape variables

Where presented, yield had positive relationships with all S-NDVI measurements (Table 4). The strongest relationship ($r = 0.81$) was for D-NDVI at GS30 in Wheat20A. The weakest relationship was S-NDVI for

Table 4

Pearson correlation coefficients between yield and tractor-based NDVI (T-NDVI), drone-based NDVI (D-NDVI) satellite-based NDVI (S-NDVI), elevation, slope, and topographic wetness index (TWI) for each field where it was collected.

Field	T-NDVI	D-NDVI GS23 ^a	D-NDVI GS30	S-NDVI GS23	S-NDVI GS30	Elevation	Slope	TWI
Barley19	0.49	NS ^b	0.41	0.45	0.40	−0.17	−0.34	0.16
Wheat19	0.28	NS	0.32	0.24	0.43	−0.17	−0.15	0.17
Wheat20A	0.68	0.74	0.81	0.73	0.77	−0.43	−0.25	0.37
Barley21	0.65	0.70	0.72	0.72	0.63	NS	−0.21	0.19
Corn Rainfed	0.31	NS	0.35	NS	0.27	NS	−0.21	0.23
Corn Irrigated	0.47	NS	0.49	NS	0.44	0.14	NS	−0.27

^a small grain growth stage 23 and 30, corn six leaf vegetative stage.

^b No significant difference at $P = 0.05$.

rainfed corn field at GS30. There were only two fields to compare GS23 small grain D-NDVI to yield, and both were fairly strong. Two additional fields could be evaluated for satellite at GS30, and they had much weaker relationships, similar to those observed in April (GS23).

Relationships between yield and landscape variables were negative for slope, although not very strong and similar to those seen for NDVI (Table 4). Field Barley19 had the strongest negative relationship between yield and slope ($r = -0.34$). Relationships for yield with elevation were mixed, with fields having no relationship and positive or negative relationships. The strongest negative relationship between yield and elevation was for Wheat20A ($r = -0.43$), which also had consistent negative relationships with NDVI and elevation across all platforms. This could have been due to the drier winter. The irrigated corn field also had a weak positive relationship between yield and elevation.

The TWI had mostly weak positive relationships with yield, even where slope had negative relationships. The strongest positive relationship for TWI and yield was Wheat20A ($r = 0.37$). The only negative relationship for TWI and yield was in the irrigated corn field, which may have been due to strong late summer storms that caused lodging in the field. This field also had a weak positive relationship between elevation and yield.

4. Discussion

4.1. Relationships between tractor, drone, and satellite NDVI

Our findings indicated that D-NDVI and T-NDVI were strongly and positively correlated, which could support D-NDVI being substituted for previously developed algorithms. However, the D-NDVI measurements were often much higher (up to 0.38 units) than the T-NDVI measurements. The S-NDVI was also always lower than D-NDVI and higher than T-NDVI in three fields (Fig. 1). While it was also suggested that D-NDVI could pick up soil background (Morris et al., 2018), the higher average values observed in our study did not align with this prior finding. This was particularly notable since T-NDVI had the lowest NDVI recorded in four out of eight fields. In another study comparing drones to a handheld active sensor, Duan et al. (2017) observed drone measurements to be 0.2 units higher, suggesting that this was due to reduced soil interference in coarser drone imagery. Soil signals also did not have a large effect on drone readings in other studies of small grains and N rates, where ground-based sensors might receive more off-nadir signals from stems (Heinemann et al., 2022). While our D-NDVI measurements had some values above 0.9 at GS30, other studies have not observed those values until heading (Guan et al., 2019; Miller and Adkins, 2021), which is another reason why high N strips are important in separating field and sensor variability.

Based on our results, it becomes evident that both soil reflectance and low biomass contributed to the reduction in T-NDVI. This reduction occurred because of the limited spatial coverage of the active sensors, which missed some field variability (Fig. 3). Tractor-mounted sensors, due to their proximity to the crop, offered high individual resolution

(0.61 m) and worked effectively when placed directly over the rows. However, accurately mapping small grain fields, especially those broadcast on the surface and tilled into the soil, would require more sensors. In contrast, drone imagery demonstrated a superior capacity to cover small grain fields, particularly when fewer sensors may be mounted on the equipment. These findings underscore the importance of field-based rather than plot-based calibrations. In field conditions, spatial variability may not align with more idealized plot conditions, as highlighted in the study by Colaço and Bramley (2018). Another issue with tractor-mounted sensors was the inclusion of NDVI measurements not used in application rates. This issue occurred in cases where the as-applied polygons represented smaller field edges or overlaps. At the same time, NDVI measurements were averaged over all active sensors. In regions of the field where biomass was consistent, T-NDVI was similar to D-NDVI, but where drainage ditches might be included, T-NDVI would be lower. This could support using aerial imagery to provide maps prior to application with the appropriate NDVI measurements. In this case, the T-NDVI may underestimate N application along field edges and overlaps.

Alternatively, S-NDVI was much closer to T-NDVI in value, potentially due to the coarser resolution of satellite imagery producing similar averages to the active tractor-mounted sensors. Nevertheless, it was important to consider whether algorithms were created by scanning rows and whether tractor-mounted sensors correctly measure small grain fields, which could indicate that S-NDVI was also less accurate in mapping field biomass.

4.2. Incorporation into algorithms

Due to the calibration from the reference strips, drone and satellite imagery were occasionally successful at predicting a similar rate to T-NDVI (Table 2). This appears to occur where at least less separation occurred between the low N and target (application zone) NDVI but always performed better when the high NDVI was at least 0.20 units higher than the target. However, in other estimates, both the drone and satellite rates were half of the active sensor platform rate and would have under-fertilized that region of the field. In these fields, D-NDVI would measure higher NDVI in low biomass regions of the field, causing it to underestimate the amount of N needed.

Over-fertilization is a concern in fields where D-NDVI and S-NDVI measurements are used. While N-rich strips can help with corrections, certain algorithms rely on NDVI cutoffs to guide N application decisions. For example, based on results from active sensors, some algorithms suggested limiting N application for NDVI values ranging from 0.2 to 0.3 (Solie et al., 2012; Thomason et al., 2011). However, as indicated in Table 2, D-NDVI and, to a lesser extent, S-NDVI might estimate higher values in specific parts of the field. Ensuring the accuracy of NDVI measurements in different field sections is crucial to avoid inappropriate N management. There are also upper limits built into algorithms, which may not take into account higher drone readings (Raun et al., 2005b; Thomason et al., 2011). Observations in Oklahoma have also noted a minimum response to N when NDVI was measured above 0.73, which

changed based on the reference strip (Raun et al., 2005a). On the other hand, many of these algorithms were based on scanning rows, i.e. the canopy (Morris et al., 2018), and the better ground coverage performed by drone measurements might still perform well within these algorithms. Other options to improve comparisons between passive and active sensors could include normalizing NDVI measurements to improve responses (Morris et al., 2018; Winterhalter et al., 2013).

One contributing factor to these discrepancies is the influence of plant distance on active sensor readings, an effect that can vary depending on plant vigor (Kipp et al., 2012). It is well known that poor plant stands can lead to underestimations of crop requirements, as noted in the case of corn (Franzen et al., 2016). To mitigate these issues, the use of drone imagery becomes valuable, as it allows for the separation of rows and the estimation of tiller and stand counts (Miller and Adkins, 2021). While D-NDVI alone may not always align with prior calibration values, its accuracy can be enhanced through the ability to perform stand counts and other spatial analyses. The use of the coefficient of variation has also been shown to correlate well with plant population (Raun et al., 2005a) and could be quickly calculated from field-wide drone (or satellite) imagery. Passive sensors such as those mounted on drones or satellites may be able to detect N along the entire canopy (Winterhalter et al., 2013), as opposed to active tractor-mounted sensors. This may explain some of the differences observed at higher biomass, although the prior study had used passive sensors just above the plant canopy (Winterhalter et al., 2013).

Satellite-based NDVI has a coarser spatial resolution than D-NDVI but also covers the entire field, which may explain why the range in NDVI was similar to that of T-NDVI. However, it did not appear to improve the chances of similar N rates (Table 2), although it has already been shown to have high enough resolution to be profitable for N application (Sozzi et al., 2021). Compared to farmer applied rates, satellite measurements of high N-reference strips have also achieved greater economic return (Mizuta et al., 2022), and satellites have not reached a plateau in NDVI as drones have (Benincasa et al., 2018).

4.3. How management, weather, and field characteristics may affect NDVI relationships

Prior studies examining plot-based comparisons may not be an accurate measure of field and annual climate variability (Colaço and Bramley, 2018). Weather may control both planting timing and seasonal growth, particularly for small grains. Some fields were not planted in the same fall window and accumulated less GDD before VR application, and differences in NDVI between platforms appear to increase with accumulated GDD. Rainfall also affected overall plant growth and varied each winter for small grains. The driest winter (2019–2020) corresponded to lower average NDVI in the field with higher elevations and steeper slopes (Wheat20A), as indicated by negative correlations with elevation and slope (Table 3). The Wheat20A field also had a weak positive correlation with TWI, indicating the importance of parts of the field that can accumulate water during drier winters. This is evident in Fig. 4C, where the Wheat20A field had several upland depressions where water could gather and higher NDVI was evident. The other small grain field observed during 2019–2020 (Wheat20B) had the lowest elevation recorded for all fields and one of the only positive relationships between NDVI and elevation observed. The only other field with this relationship (Barley21) had higher elevations and gentler slopes but also a lower TWI range. However, visual drone imagery revealed a drainage pattern across the field where reduced growth was occurring (Fig. 4E), so that higher elevations may provide more stable slopes for plant growth (Fig. 3).

Excess winter rainfall might also reduce small grain growth, which was evident in the imagery for field Wheat19, where the farmer performed 0N application in depressional Delmarva Bays (Fig. 4A). The removal of lower elevation depressions from T-NDVI might explain why there was no relationship with elevation, although it was present for D-NDVI and S-NDVI. The other field flown that season, Barley19, had

strong negative relationships with both elevation and slope (Fig. 4B). While Barley19 had a similar range in slope to Wheat19, the elevation contours revealed longer regions of steeper slopes with lower NDVI values. Overall, slope had stronger negative relationships with NDVI across all platforms, which indicates the difficulty in growing small grains on Delmarva. Even in a year with more moisture, slopes on Barley19 may have caused more runoff and reduced growth, as evidenced by the reliance on TWI for higher NDVI. During the 2018–2019, depressions in Wheat19 suffered crop failure due to excess water accumulation, whereas an adjacent field (Barley19) exhibited higher NDVI in areas with moisture collection and lower NDVI in regions prone to erosion and runoff. The Barley21 field had gentler slopes, and the stability appeared to lead to more consistent NDVI, while the gullies cutting across the field had lower NDVI (Fig. 4E). Where corn was planted in this field in 2020 (Fig. 4A), there was more variability in NDVI along these slopes, but the wider gully still had the lowest NDVI. Alternatively, the irrigated corn field had a range of slopes, ditches, and depressions but a more consistent NDVI map, indicating how reducing the limitations of moisture produced a more even stand across the field. This suggests the need for better management of Delmarva, which would include landscape variables (management zones), irrigation, and weather for VR applications.

The only consistent factor among landscape characteristics and measured NDVI was the variability across the fields. Even though the slope was consistently negative, the relationship was either weak or not significant in most fields, while elevation sometimes boosted NDVI, and at other times, it reduced it. The use of both high N reference strips with management zones and weather conditions could improve N management for Delmarva sensor-based N applications (Tagarakis and Ketterings, 2018; Thompson and Puntel, 2020).

4.4. How management, weather, and field characteristics may affect yield relationships

Yield had positive relationships with NDVI across all platforms and fields, which is expected, as NDVI is a proxy for biomass (Raun et al., 2001). However, these NDVI measurements were made prior to reproductive stages and VRN application. For small grains and corn, vegetation indices typically have their strongest relationship at the beginning of reproductive stages (Miller et al., 2022; Naser et al., 2020). Stronger relationships prior to reproductive stages might indicate that spring management had little effect, and earlier season stress had already reduced yield potential (Table 4). There were some fields, such as the Wheat19 and the rainfed corn field, which had weaker relationships between yield and NDVI when NDVI was measured at sidedress. However, the small grain fields (Wheat20A and Barley21) and the irrigated corn field all had stronger relationships at sidedress, with Wheat20A having an r of 0.81 between yield and D-NDVI at GS30.

The Wheat20A field also had high correlations between T-NDVI and S-NDVI (r ranged from 0.72 to 0.74) during the winter (GS23) months by both drone and satellite, indicating that little change in yield potential occurred after that point. This was compared to fields Wheat19 and Barley19, with r values of 0.24 and 0.45 by satellite, respectively. For Wheat20A, it appeared that the N application did very little to change yield, and landscape variables might have been more important, although we did not have NDVI measurements following sidedress application to compare. However, the stronger relationships between D-NDVI or S-NDVI with yield at GS23 might explain why Wheat20A had the strongest negative relationship between elevation and yield and the strongest positive relationship with TWI (Table 4). In that field, wheat growth was probably related to soil moisture content, which had been drier that winter. These conditions were probably more limiting than N and were supported by the need for algorithms to be adapted for weather conditions (Tagarakis and Ketterings, 2018). The Barley21 field also had higher correlations between yield and NDVI in both GS23 and GS30 but

may have been related to the slopes or drainage regions that limited growth, since elevation increased biomass based on NDVI measurements but had no relationship to yield. We do not have enough information to confirm whether growth was limited at planting or later in the season, as rainfall in the region was similar to that in the first year of the study. However, prior studies in calibration strips and active sensors observed that N applied before GS30 should catch up with low N issues (Raun et al., 2008), which suggested that these fields might have had other limiting factors that sensor-based N application could not correct. Under irrigated conditions, small grains have weaker correlations between yield and NDVI (Naser et al., 2020). Drone and satellite imagery may provide similar information when observing field and weather conditions, with limiting or excessive moisture providing the field variability necessary to decide management practices.

5. Conclusions

Relationships among T-NDVI, D-NDVI, and S-NDVI were positively correlated and had a moderately strong linear regression. Even though they were correlated, D-NDVI measurements were always higher than T-NDVI and S-NDVI. The higher NDVI measurements obtained from the drone helped explain its capability to predict lower N rates compared to T-NDVI, and this trend was sometimes observed in S-NDVI as well. This phenomenon was influenced by soil reflectance and was further compounded by the fact that the T-NDVI sensors did not achieve complete ground coverage. This implies that S-NDVI and D-NDVI may provide better estimates of field variability. Studies of N-rate vs. drone imagery may provide better calibrations for algorithms, as well as include landscape factors for management. The D-NDVI and S-NDVI helped reveal how landscape variables contributed to both yield and N-rate differences, further suggesting that algorithms needed adjustments based on longer plot lengths that included greater field variability. A major benefit of using drone or satellite imagery was the ability to obtain measurements easily over the entire growing season, as opposed to only running a tractor-based sensor on the day of application. Multiple measurements allowed NDVI to be used to map different weather and soil conditions that could better predict the response to any VR applications.

Abbreviations

DSM	digital surface model
GDD	growing degree days
GS23	growth stage 23
GS30	growth stage 30
NDRE	normalized difference red edge
NDVI	normalized difference vegetation index
TWI	topographic wetness index
VR	variable rate
VRN	variable rate nitrogen

Availability of data and materials

Data are available upon request by the readers.

Authors' contributions

J.M.: conception of the project, collection of drone and tractor data, analyses and first draft of manuscript; P.M.: consulting on project, editing of draft; and M.S.: collection of satellite imagery, analyses and editing of draft.

Declaration of competing interest

The authors of this manuscript declare no conflict of interest or competing interest.

Acknowledgments

We would like to acknowledge our Maryland farmer cooperators and Shawn Tingle for his assistance in the field. We acknowledge the support provided by the Harry R. Hughes Center for Agro-Ecology. The funders had no role in study design, data collection and analysis, decision to publish or preparation of the manuscript.

References

- Ator, S.W., Blomquist, J.D., Webber, J.S., Chanut, J.G., 2020. Factors driving nutrient trends in streams of the Chesapeake Bay watershed. *J. Environ. Qual.* 49, 812–834.
- Aula, L., Omara, P., Nambi, E., Oyebyi, F.B., Raun, W.R., 2020. Review of active optical sensors for improving winter wheat nitrogen use efficiency. *Agronomy* 10, 1157.
- Barker, D.W., Sawyer, J.E., 2010. Using active canopy sensors to quantify corn nitrogen stress and nitrogen application rate. *Agron. J.* 102, 964–971.
- Barker, D.W., Sawyer, J.E., 2012. Using active canopy sensing to adjust nitrogen application rate in corn. *Agron. J.* 104, 926–933.
- Beegle, D., 2013. Nutrient management and the Chesapeake Bay. *J. Contemp. Wat. Res. Educ.* 151, 3–8.
- Benincasa, P., Antognelli, S., Brunetti, L., Fabbri, C.A., Natale, A., Sartoretti, V., Modeo, G., Guiducci, M., Tei, F., Vizzari, M., 2018. Reliability of NDVI derived by high resolution satellite and UAV compared to in-field methods for the evaluation of early crop N status and grain yield in wheat. *Exp. Agric.* 54, 604–622.
- Cao, Q., Miao, Y., Feng, G., Gao, X., Liu, B., Liu, Y., Li, F., Khosla, R., Mulla, D.J., Zhang, F., 2017. Improving nitrogen use efficiency with minimal environmental risks using an active canopy sensor in a wheat-maize cropping system. *Field Crops Res.* 214, 365–372.
- Colaco, A.F., Bramley, R.G., 2018. Do crop sensors promote improved nitrogen management in grain crops? *Field Crops Res.* 218, 126–140.
- Dellinger, A.E., Schmidt, J.P., Beegle, D.B., 2008. Developing nitrogen fertilizer recommendations for corn using an active sensor. *Agron. J.* 100, 1546–1552.
- Duan, T., Chapman, S.C., Guo, Y., Zheng, B., 2017. Dynamic monitoring of NDVI in wheat agronomy and breeding trials using an unmanned aerial vehicle. *Field Crops Res.* 210, 71–80.
- Erdle, K., Mistele, B., Schmidhalter, U., 2011. Comparison of active and passive spectral sensors in discriminating biomass parameters and nitrogen status in wheat cultivars. *Field Crops Res.* 124, 74–84.
- Fassa, V., Pricca, N., Cabassi, G., Bechini, L., Corti, M., 2022. Site-specific nitrogen recommendations' empirical algorithm for maize crop based on the fusion of soil and vegetation maps. *Comput. Electron. Agric.* 203, 107479.
- Franzen, D., Kitchen, N., Holland, K., Schepers, J., Raun, W., 2016. Algorithms for in-season nutrient management in cereals. *Agron. J.* 108, 1775–1781.
- Guan, S., Fukami, K., Matsunaka, H., Okami, M., Tanaka, R., Nakano, H., Sakai, T., Nakano, K., Ohdan, H., Takahashi, K., 2019. Assessing correlation of high-resolution NDVI with fertilizer application level and yield of rice and wheat crops using small UAVs. *Remote Sens.* 11, 112.
- Heinemann, P., Haug, S., Schmidhalter, U., 2022. Evaluating and defining agronomically relevant detection limits for spectral reflectance-based assessment of N uptake in wheat. *Eur. J. Agron.* 140, 126609.
- Holland, K.H., Lamb, D.W., Schepers, J.S., 2012. Radiometry of proximal active optical sensors (AOS) for agricultural sensing. *IEEE J. Sel. Top. Appl. Earth Observ. Remote Sens.* 5, 1793–1802.
- Holland, K.H., Schepers, J.S., 2010. Derivation of a variable rate nitrogen application model for in-season fertilization of corn. *Agron. J.* 102, 1415–1424.
- Imap, M.D., 2022. LiDAR DEM Maps by County. <https://imap.maryland.gov/pages/lidar-download>.
- Inman, D., Khosla, R., Mayfield, T., 2005a. On-the-go active remote sensing for efficient crop nitrogen management. *Sens. Rev.* 25, 209–214.
- Inman, D., Khosla, R., Westfall, D.G., Reich, R., 2005b. Nitrogen uptake across site specific management zones in irrigated corn production systems. *Agron. J.* 97, 169–176.
- Kipp, S., Mistele, B., Schmidhalter, U., 2012. Active sensor performance-dependence on measuring height, device temperature and light intensity. In: Stafford, J., Schepers, J., Carter, P. (Eds.), 11th International Conference on Precision Agriculture. Indianapolis, USA, pp. 15–18.
- Miller, J.O., Adkins, J., 2021. Monitoring winter wheat growth at different heights using aerial imagery. *Agron. J.* 113, 1586–1595.
- Miller, J.O., Shober, A.L., VanGessel, M.J., 2022. Post-harvest drone flights to measure weed growth and yield associations. *Agric. Env. Lett.* 7, e20081.
- Mizuta, K., Morales, A.C., Lacerda, L.N., Miao, Y.X., Cammarano, D., Coulter, J.A., Nielsen, R.L., Gunzenhauser, R., McArtor, B., Kuehner, K., Wakahara, S., Mulla, D.J., Quinn, D.J., 2022. Evaluating a satellite remote sensing and calibration strip-based precision nitrogen management strategy for maize in Minnesota and Indiana. In: Proceedings of the 15th International Conference on Precision Agriculture. Minneapolis, USA, pp. 1–9.
- Morris, T.F., Murrell, T.S., Beegle, D.B., Camberato, J.J., Ferguson, R.B., Grove, J., Ketterings, Q., Kyvergy, P.M., Laboski, C.A., McGrath, J.M., Meisinger, J.J., Melkonian, J., Nafziger, E.D., Osmond, D., Sawyer, J.E., Scharf, P.C., Smith, W., Spargo, J.T., van Es, H.M., Yang, H.S., 2018. Strengths and limitations of nitrogen rate recommendations for corn and opportunities for improvement. *Agron. J.* 110, 1–37.
- Naser, M.A., Khosla, R., Longchamps, L., Dahal, S., 2020. Using NDVI to differentiate wheat genotypes productivity under dryland and irrigated conditions. *Remote Sens.* 12, 824.

- Raun, W.R., Solie, J.B., Johnson, G.V., Stone, M.L., Lukina, E.V., Thomason, W.E., Schepers, J.S., 2001. In-season prediction of potential grain yield in winter wheat using canopy reflectance. *Agron. J.* 93, 131–138.
- Raun, W.R., Solie, J.B., Martin, K.L., Freeman, K.W., Stone, M.L., Johnson, G.V., Mullen, R.W., 2005a. Growth stage, development, and spatial variability in corn evaluated using optical sensor readings. *J. Plant Nutr.* 28, 173–182.
- Raun, W.R., Solie, J.B., Stone, M.L., Martin, K.L., Freeman, K.W., Mullen, R.W., Zhang, H., Schepers, J.S., Johnson, G.V., 2005b. Optical sensor-based algorithm for crop nitrogen fertilization. *Commun. Soil Sci. Plant Anal.* 36, 2759–2781.
- Raun, W.R., Solie, J.B., Taylor, R.K., Arnall, D.B., Mack, C.J., Edmonds, D.E., 2008. Ramp calibration strip technology for determining midseason nitrogen rates in corn and wheat. *Agron. J.* 100, 1088–1093.
- Roberts, D.F., Kitchen, N.R., Scharf, P.C., Sudduth, K.A., 2010. Will variable-rate nitrogen fertilization using corn canopy reflectance sensing deliver environmental benefits? *Agron. J.* 102, 85–95.
- Samborski, S.M., Tremblay, N., Fallon, E., 2009. Strategies to make use of plant sensors-based diagnostic information for nitrogen recommendations. *Agron. J.* 101, 800–816.
- Solie, J.B., Monroe, A.D., Raun, W.R., Stone, M.L., 2012. Generalized algorithm for variable-rate nitrogen application in cereal grains. *Agron. J.* 104, 378–387.
- Sozzi, M., Kayad, A., Gobbo, S., Cogato, A., Sartori, L., Marinello, F., 2021. Economic comparison of satellite, plane and UAV-acquired NDVI images for site-specific nitrogen application: observations from Italy. *Agronomy* 11, 2098.
- Stadler, A., Rudolph, S., Kupisch, M., Langensiepen, M., van der Kruk, J., Ewert, F., 2015. Quantifying the effects of soil variability on crop growth using apparent soil electrical conductivity measurements. *Eur. J. Agron.* 64, 8–20.
- Tagarakis, A.C., Ketterings, Q.M., 2018. Proximal sensor-based algorithm for variable rate nitrogen application in maize in northeast U.S.A. *Comput. Electron. Agric.* 145, 373–378.
- Thompson, L.J., Puntel, L.A., 2020. Transforming unmanned aerial vehicle (UAV) and multispectral sensor into a practical decision support system for precision nitrogen management in corn. *Remote Sens.* 12, 1597.
- Thomason, W.E., Phillips, S.B., Davis, P.H., Warren, J.G., Alley, M.M., Reiter, M.S., 2011. Variable nitrogen rate determination from plant spectral reflectance in soft red winter wheat. *Precis. Agric.* 12, 666–681.
- Walsh, O.S., Shafian, S., Marshall, J.M., Jackson, C., McClintick-Chess, J.R., Blanscet, S.M., Swoboda, K., Thompson, C., Belmont, K.M., Walsh, W.L., 2018. Assessment of UAV based vegetation indices for nitrogen concentration estimation in spring wheat. *Adv. Remote Sens.* 7, 71–90.
- Winterhalter, L., Mistele, B., Schmidhalter, U., 2013. Evaluation of active and passive sensor systems in the field to phenotype maize hybrids with high-throughput. *Field Crops Res.* 154, 236–245.
- Yu, J., Wang, J., Leblon, B., Song, Y., 2021. Nitrogen estimation for wheat using UAV-based and satellite multispectral imagery, topographic metrics, leaf area index, plant height, soil moisture, and machine learning methods. *Nitrogen* 3, 1–25.